HNPS Advances in Nuclear Physics

Vol 16 (2008)

HNPS2008

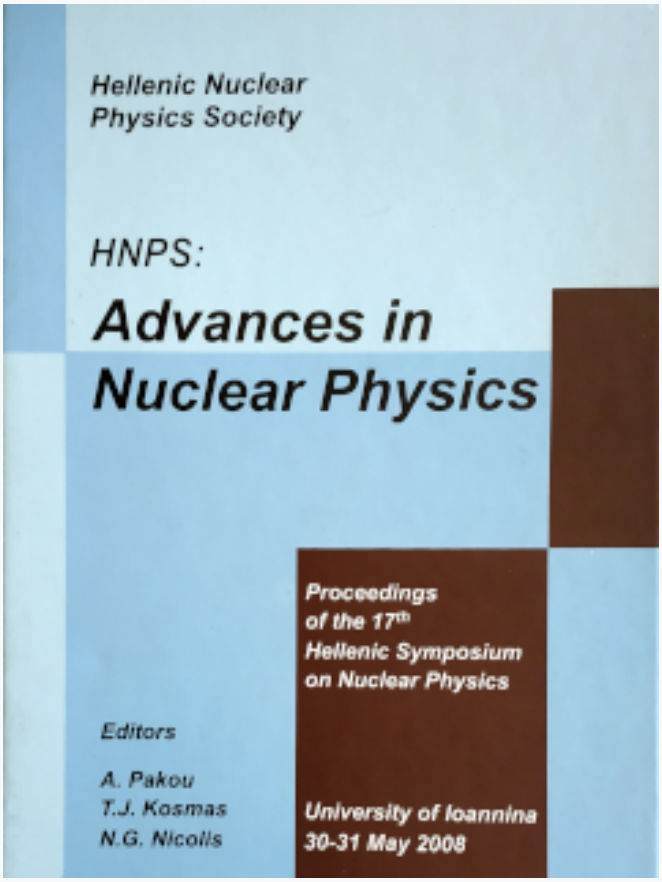

Barrier curvatures and positions for weakly and strongly bound nuclei

K. Zerva, A. Pakou

doi: 10.12681/hnps.2604

Barrier curvatures and positions for weakly and strongly bound nuclei

K. Zerva [a], A. Pakou [a],

[a] *Department of Physics, University of Ioannina, 45110 Ioannina, Greece*

Abstract

Barrier curvatures as a function of the potential diffusivity, for weakly and strongly bound nuclei, are studied via elastic scattering data at near barrier energies for ^{6,7}Li and ^{14}N-^{16}O on silicon . A parametrization of curvature as a function of diffusivity is given and critical distances for the barrier position are determined. The results indicate similar behaviour for both weakly and strongly bound projectiles. Additionally, by studing total reaction cross sections for ^{6}Li and ^{7}Li on silicon targets, curvatures and barrier locations are determined at near barrier energies. The results indicate a stronger absorption for ^{6}Li than for ^{7}Li.

Fusion is a popular subject for several decades revisited nowdays with the study of weakly bound stable or radioactive systems. Systematic studies of experimental fusion excitation functions have resulted in parametrizations of the barrier radius and height. For interpreting fusion data, and/or predicting fusion cross sections, both simplified and realistic coupled channel codes have been used. Energy-independent Woods Saxon (WS) form for the real nuclear potential are used:

$$V_N(r) = -\frac{V_0}{1 + exp(\frac{r-R_S}{\alpha})} \quad (1)$$

Above barrier excitation functions have been reproduced by simply optimizing the diffusivity α whilst constraining the barrier height to experimental values [1]. The arosen question is if these diffusivities can describe well elastic scattering data and total reaction cross sections.

In this paper we study the evolution of barrier widths and diffusivities for 4 systems, two of them with weakly bound projectiles and two with well bound projectiles while using the same target. Elastic scattering data at near barrier energies are analysed for ^{6}Li+^{28}Si, ^{7}Li+^{28}Si, ^{14}N+^{28}Si and ^{16}O+^{28}Si [2–4]

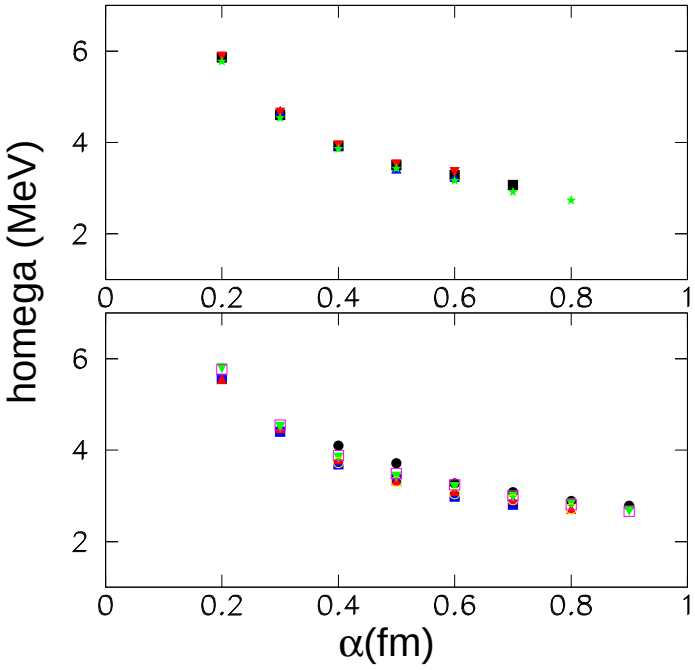

Fig. 1. The evolution of the barrier curvature ($\hbar\omega$ as a function of the potential diffusivity for ^{6}Li+^{28}Si (top) and ^{7}Li+^{28}Si (bottom), at several barrier energies.

by using a Wood-Saxon potential. Fits are performed for various values of diffusivities keeping $\alpha_v = \alpha_w$ for the best value of $r_v = r_w$ for all diffusivities, obtained before, and handling V_0 and W_0 as free parameters. The results, in fact the curvatures ($\hbar\omega$) of the best fitted potentials to the elastic scattering data, as a function of the diffusivity α, are shown in Figures 1 and 2. We point out a similar behaviour for both weakly and strongly bound projectiles while in all cases the energy dependence is weak. We should mention that the analyzed data refer to the energy regime of $E/E_{C.b.} \sim$ 1-1.5. To obtain a systematic description-parametrization of curvatures as a function of diffusivity, we proceed as follows.

Since the elastic scattering is sensitive to the tail of the potential we can write equation (1) at large distances as

$$V_N(r) = V_N(R_B) exp(-\frac{r - R_B}{\alpha}) \qquad (2)$$

where R_B is the position of the barrier. At R_B the derivative of the total

projectile	$\hbar\omega$(MeV)	R_B(fm)	$r_0(fm)$	$R_B{}^C$(fm)
^{6}Li	$22.61((R_B\ \sqrt{\alpha})^{-1}$ -$\sqrt{\alpha}R_B{}^{-2})$	8.62	1.78	7.90
^{7}Li	$21.24((R_B\ \sqrt{\alpha})^{-1}$ -$\sqrt{\alpha}R_B{}^{-2})$	8.56	1.73	8.01
^{14}N	$25.06((R_B\ \sqrt{\alpha})^{-1}$ -$\sqrt{\alpha}R_B{}^{-2})$	9.60	1.76	8.55
^{16}O	$25.73((R_B\ \sqrt{\alpha})^{-1}$ -$\sqrt{\alpha}R_B{}^{-2})$	10.20	1.84	8.66

Table 1
The parametrization of $\hbar\omega$ as a function of the diffusivity for well and weakly bound projectiles. The barrier position R_B was handled as a free parameter and it was found to obey the relation R_B= 1.78 ($A_p{}^{1/3}$+$A_T{}^{1/3}$) fm . For comparison reasons the barrier location according to Christensen [5], $R_B{}^C$= 1.07 ($A_p{}^{1/3}$+$A_T{}^{1/3}$) + 2.72 fm is also given.

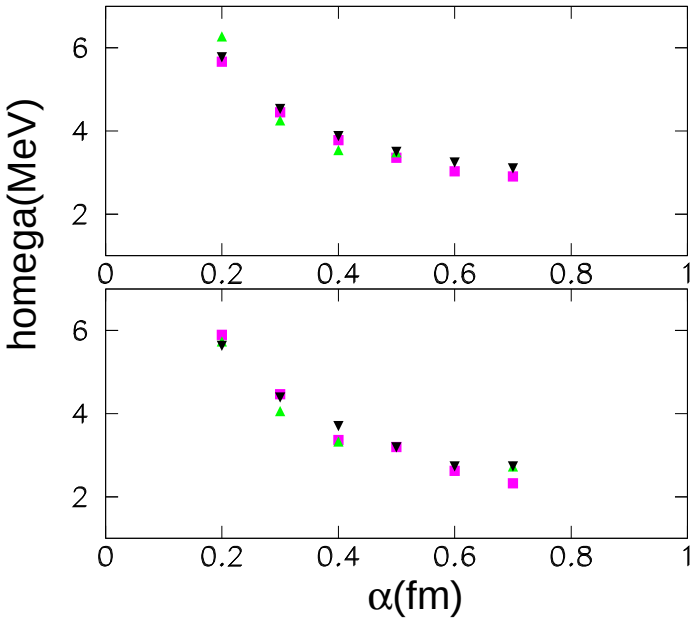

Fig. 2. The evolution of the barrier curvature ($\hbar\omega$ as a function of the potential diffusivity for ^{14}N+^{28}Si (top) and ^{16}O+^{28}Si (bottom), at several barrier energies.

potential V=V_N+V_C must vanish and thus

$$V'(R_B) = -\frac{1}{\alpha}V_N(R_B) - \frac{Z_p Z_T e^2}{R_B^2} = 0 \qquad (3)$$

projectile	V_B(MeV)	R_B(fm)	$\hbar\omega$(MeV)	α(fm)
^{6}Li	6.49	8.80	4.00	0.46
^{7}Li	6.55	9.02	3.19	0.68

Table 2
Best fitted parameters (V_B, R_B, $\hbar\omega$) to the total reaction cross section data. Diffusivites have been extracted via equation (8) - see Table I.

and

$$V_N(r) = \frac{Z_p Z_T e^2 \alpha}{R_B^2} exp(-\frac{r - R_B}{\alpha}) \tag{4}$$

Taking into account a parabolic approximation of the potential at the top pf the Coulomb barrier

$$V(r) = V_B - \frac{1}{2}\mu\omega^2(r - R_B)^2 \tag{5}$$

and by using equation (4) we obtain for the curvature of the potential

$$\mu\omega^2 = -(V_N' + V_C') = \frac{Z_p Z_T e^2}{\alpha R_B^2}(1 - \frac{2\alpha}{R_B}) \tag{6}$$

and

$$\hbar\omega = \hbar\sqrt{\frac{Z_p Z_T e^2}{\mu\alpha R_B^2}(1 - \frac{2\alpha}{R_B})} \tag{7}$$

Applying a Taylor expansion in the second part of the equation and keeping the first two terms we obtain

$$\hbar\omega = \frac{A}{\sqrt{\alpha}} - B\sqrt{\alpha} \tag{8}$$

where A and B are functions of R_B

$$A = \frac{\hbar}{R_B}\sqrt{\frac{Z_p Z_T e^2}{\mu}} \;\; and \;\; B = \frac{\hbar}{R_B^2}\sqrt{\frac{Z_p Z_T e^2}{\mu}} \tag{9}$$

From equation (8) and (9) we see that the curvature $\hbar\omega$ is a function of $\sqrt{\alpha}$ with only unknown the barrier position R_B. Therefore the data displayed in Figures 1 and 2 can be fitted with a function of the form of equation (8), handling R_B as a free parameter. The results of the fit are included in Table I.

Barrier positions are found amongst themselves in good compatibility as long as we express this radius as

$$R_B = r_0(A_p^{1/3} + A_T^{1/3}) \sim 1.78(A_p^{1/3} + A_T^{1/3})fm \tag{10}$$

but not found in consistency with the Christensen parametrization

$$R_B = 1.07(A_p^{1/3} + A_T^{1/3}) + 2.73fm \tag{11}$$

Subsequently we will focus on the analysis of total reaction cross sections obtained previously [6,7] at near barrier energies (0.8 to 1.5 $E_{C.b.}$) for ^{6,7}Li+^{28}Si. The data were analysed by using the Wong formula [8]

$$\sigma_R = \frac{\hbar\omega R_B^2}{2E_{c.m}} ln\left[1 + exp\left(\frac{2\pi}{\hbar\omega}[E_{c.m} - V_B]\right)\right] \tag{12}$$

where $\hbar\omega$ is the curvature of the potential V_b is the barrier height, and R_B the radius of the potential at barrier. A best fit to these data as a function of energy, with free parameters V_B, R_B and $\hbar\omega$ are performed and the results are presented in Table II. From the obtained curvatures, shown in Table 2, it is obvious that for ^{6}Li the tunneling time is shorter than for ^{7}Li, or that ^{6}Li is more absorptive than ^{7}Li. This is also the conclusion from elastic scattering in ^{27}Al at much higher energies ($E \sim 10E_{C.B.}$) observed by Cook et al. [9]. In this respect it is expected that fusion cross sections for ^{6}Li on silicon will be larger than for ^{7}Li, a fact which remains to be proved. The corresponding diffusivities to these curvatures, extracted via the parametrization obtained before from elastic scattering data is also displayed in Table II. These diffusivities give very good fits to the elastic scattering data. This result seems to confirm the one quoted in [10] that for near spherical nuclei small diffusivities $\sim$0.6 can describe both elastic scattering and fusion data.

Summarizing, we have analyzed available elastic scattering data for weakly and strongly bound projectiles in ^{28}Si and total reaction cross sections for ^{6,7}Li+^{28}Si at near barrier energies. The curvatures of the potential as a function of the surface diffusness were parametrized via the barrier radius. The barrier location, via this parametrization was found similar for both weakly and strongly bound projectiles, while is found compatible with the value $R_B \sim 1.78(A_p{}^{1/3} + A_T{}^{1/3})$. The analysis of the total cross sections gives potential parameters compatible with the elastic scattering results, while the obtained curvatures indicate a stronger absorption for ^{6}Li than for ^{7}Li compatible with previous findings.

References

[1] M. Dasgupta et al., Annu. Rev. Nucl. Part. Sci. **48**, 401 (19980 and references therein.

[2] A. Pakou et al., Phys. Lett. **B 556**, 21 (2003).

[3] A. Pakou et al., Phys. Rev. **C 69**, 054602 (2004).

[4] J.S. Eck, T.J. Gray, and R.K Gardner, Phys. Rev. **C 16**, 1873(1977)

[5] P. R. Christensen, and A. Winther, Phys. Lett. **B 65**, 19(1976).

[6] A. Pakou et al. Nucl. Phys. **A 784**,13 (2007)

[7] A. Pakou et al., submitted for publication in PRC.

[8] C. W. Wong, Phys. Rev. Lett. **31**, 766 (1973).

[9] J. Cook, J. M. Clarke and R. J. Griffiths, J. Phys. G: Nucl. Phys. **6**, 1251(1980).

[10] K. Washiyama, K. Hagino, and M. Dasgupta, Phys. Rev. **C73**, 034607 (2006).